Journal of Alloys and Compounds 509 (2011) 8573–8576

Contents lists available at ScienceDirect

Journal of Alloys and Compounds

journal homepage: www.elsevier.com/locate/jallcom

An open aperture z-scan study of Sr_2CeO_4 blue phosphor

R. Seema [a], C.S. Suchand Sandeep [c], Reji Philip [c], Nandakumar Kalarikkal [a,b,*]

[a] School of Pure and Applied Physics, Mahatma Gandhi University, Kottayam 686 560, Kerala, India
[b] Centre for Nanoscience and Nanotechnology, Mahatma Gandhi University, Kottayam 686 560, Kerala, India
[c] Light and Matter Physics Group, Raman Research Institute, Bangalore 560 080, Karnataka, India

ARTICLE INFO

Article history:
Received 3 January 2011
Received in revised form 1 June 2011
Accepted 7 June 2011
Available online 15 June 2011

Keywords:
Sr_2CeO_4
Phosphors
Luminescence
X-ray diffraction
HRTEM
z-Scan

ABSTRACT

Sr_2CeO_4 blue phosphor has been prepared by the solid-state reaction method. The X-ray diffraction (XRD) study confirms the structure of the system to be orthorhombic. High resolution electron transmission microscopy reveals that Sr_2CeO_4 prepared by the solid state reaction method is composed of elongated spherical structures of length ~0.2–0.6 μm and width ~90–150 nm. The excitation spectrum shows a broad band which peaks at 275 nm. The emission spectrum shows a broad band which peaks at 467 nm when excited at 275 nm. The emission band is assigned to the energy transfer between the molecular orbital of the ligand and charge transfer (CT) state of the Ce^{4+} ion. The Commission International de l'Eclairage (CIE) co-ordinates are $x = 0.15$, and $y = 0.23$. The nonlinear absorption behavior of Sr_2CeO_4 has been investigated using the open aperture z-scan technique. The calculated effective two-photon absorption coefficient shows that the Sr_2CeO_4 blue phosphor is a promising optical limiting material.

1. Introduction

Non-linear optical (NLO) phenomena in many systems have been the subject of considerable interest in recent years for potential applications in optical switches, filters, waveguides and electro-optic devices. The z-scan method [1] has become a popular method for measurements of optical nonlinearities, particularly nonlinear refraction and nonlinear absorption [2,3]. For a medium with nonlinear refraction as well as nonlinear absorption, a z-scan measurement without aperture (open-aperture z-scan) is usually used to obtain the nonlinear absorption coefficient [4–6].

In 1998, Danielson reported the blue luminescence of Sr_2CeO_4 prepared by the combinatorial techniques [7]. The structure of Sr_2CeO_4 is reported to have orthorhombic crystal symmetry. The structure of Sr_2CeO_4 contains one dimensional chains of edge sharing CeO_6 octahedron linked together by strontium ions [8]. Further research suggested that the blue emission of Sr_2CeO_4 originates from the metal-to-ligand charge transfer (CT) transition in which Ce^{4+} and O^{2-} ions act as the metal and ligand respectively [9,10]. This phosphor exhibits blue-white luminescence efficiently under excitation with UV light, cathode ray or X-ray.

The nonlinear optical properties of Sr_2CeO_4 have not been investigated previously. We report our investigations on structural and optical characterization performed on Sr_2CeO_4 blue phosphor synthesized by solid-state reaction method.

2. Materials and methods

The Sr_2CeO_4 phosphor was synthesized by the conventional solid-state reaction method. The starting materials were $SrCO_3$ (CDH, 99% purity) and CeO_2 (Indian Rare Earths, 99% purity). Stoichiometric compositions of the starting materials were taken to prepare Sr_2CeO_4. The composition was thoroughly homogenized in an agate mortar for 5 h in the presence of acetone. The sample was dried at room temperature and then transferred to quartz crucibles for heat treatment at 1000 °C for 36 h in the air, finally cooled to room temperature by the furnace shut off.

The crystal structure and phase of the phosphor were analyzed using a Phillips X'Pert Pro XRD with Cu-Kα radiation (1.54056 Å). Step scanned powder XRD data was collected in the 2θ range 10–80° with a step size of 0.02 and a scan speed of 0.5 s per step at room temperature (25 °C) on the finely ground sample. Transmission electron microscopy (TEM) has been performed using JEOL JEM 3010 operated at 200 kV accelerating voltage. High resolution transmission electron microscopy (HRTEM) analysis was used to image crystallite size. Selected Area Electron Diffraction (SAED) pattern of the sample was also taken. The absorption spectrum was taken using a UV–Vis spectrophotometer (SHIMADZU, UV-2450). Photoluminescence measurements at room temperature were performed using a spectrofluorophotometer (SHIMADZU, RF-5301PC). A 150 W xenon lamp was used as the excitation source and the emission slit width was 1.5 nm.

The open aperture z-scan [1] experiment was employed to measure the nonlinear transmission of the Sr_2CeO_4 sample suspended in di-ethylene glycol. Here a laser beam is used for sample excitation, and its propagation direction is considered as the z-axis. The beam is focused using a convex lens and the focal point is taken as $z = 0$. The beam has maximum energy density at the focus, which will symmetrically reduce towards either side on the z-axis. In the experiment, the sample is placed in the beam at different positions with respect to the focus (i.e., scanned on the z-axis), and the corresponding transmissions are measured. Thus, the obtained position–transmission curve is the open aperture z-scan curve. From this curve the nonlinear absorption coefficient of the sample can be calculated.

---

* Corresponding author. Tel.: +91 481 2731043.
E-mail address: nkkalarikkal@yahoo.com (N. Kalarikkal).

0925-8388/$ – see front matter © 2011 Elsevier B.V. All rights reserved.
doi:10.1016/j.jallcom.2011.06.019

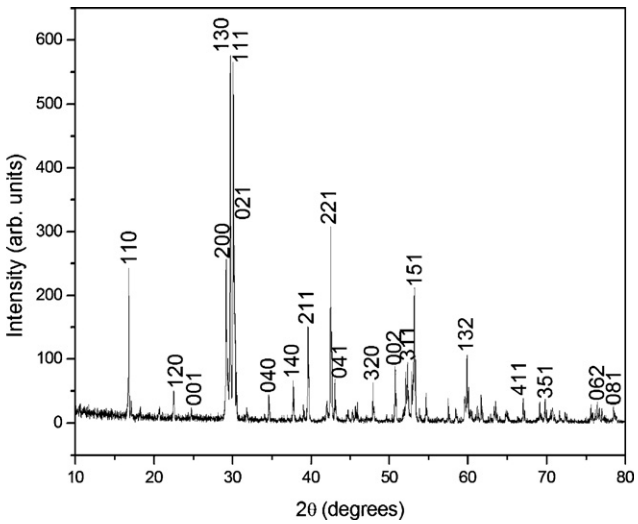

Fig. 1. The XRD pattern of Sr_2CeO_4.

Since the sample sees different laser intensities at each position, this position dependent transmission can be easily scaled to its intensity dependent transmission. For instance, for an incident Gaussian beam of wavelength λ, the beam radius at position z is given by $\omega(z) = \omega(0)[1 + (z/z_0)^2]^{1/2}$ where $\omega(0)$ is the focal spot radius and z_0 is the Rayleigh range given by $\pi\ \omega(0)^2/\lambda$. Therefore knowing the energy of laser pulse, the input laser fluence and intensity can be calculated for each z value.

Our automated z-scan setup used a precision stepper motor controlled translation stage to move the sample along the z-direction. The sample taken in a 1 mm cuvette was translated along the beam axis through the focal region over a distance substantially longer than the Rayleigh range. The sample suspension was prepared such that the linear transmittance is 70% at 532 nm. Of the two pyroelectric energy probes (Rj7620, Laser Probe Inc.) used, one monitored the input energy, while the other monitored the transmitted energy through the sample. The frequency-doubled output (532 nm) of a Q-switched Nd:YAG laser (Minilite, Continuum Inc.) was used for exciting the sample. The laser pulse width was 5 ns (FWHM). The laser pulse energy used for the experiments was 100 μJ. The pulses were fired in the "single shot" mode, allowing sufficient time between successive pulses (more than 1 s) to avoid accumulative thermal effects in the sample.

3. Results and discussion

3.1. Structural characterization

Fig. 1 shows the XRD pattern of Sr_2CeO_4 phosphor. Entire diffraction peaks in the pattern were correctly indexed to JCPDS Card No: 50-0115, which confirms the orthorhombic crystal structure to Sr_2CeO_4. By employing the software XRDA 3.1, we obtained the cell parameters of Sr_2CeO_4 as $a = 6.11$ Å, $b = 10.35$ Å and $c = 3.60$ Å and are consistent with the previously reported data [7,8].

Table 1
A mutual comparison between the values obtained from the experimental peaks of XRD, JCPDS data, and the values obtained from the FFT of the TEM.

XRD (experimental data) 2θ (°)	JCPDS values			*d*-Spacing values obtained from the FFT of TEM (Å)
	2θ (°)	*h k l*	*d*-spacing (Å)	
16.84	16.82	1 1 0	5.28	5.27
29.19	29.17	2 0 0	3.06	3.07
29.75	29.70	1 3 0	3.01	2.97
30.06	30.06	1 1 1	2.97	
30.27	30.24	0 2 1	2.95	2.75
39.60	39.61	2 1 1	2.27	2.25
42.56	42.51	2 2 1	2.13	2.10
53.18	53.16	1 5 1	1.72	1.73
59.90	59.89	1 3 2	1.54	1.51

Fig. 2(a) shows the TEM image of Sr_2CeO_4, which clearly gives evidence of the size of the crystal formed. It consists of elongated spherical structures with length of ~0.2–0.6 μm and width of ~90–150 nm. Fig. 2(b) shows the HRTEM image with lattice fringes corresponding to different inter-planar distances. The inset shows the FFT of Fig. 2(b). The FFT image was used to calculate various inter-planar distances and the values obtained are tabulated in Table 1 along with the XRD peaks and JCPDS values. By comparison, the formation of Sr_2CeO_4 phase is confirmed.

3.2. Optical characterization

Fig. 3(a) shows the UV–Vis absorption spectrum of pure Sr_2CeO_4 phosphor. There is no absorption between 450 and 850 nm, indicating the high transparency of the sample in the visible region. The UV–Vis absorption spectrum of pure Sr_2CeO_4 is composed of two absorption peaks centering around 275 nm (4.52 eV) and 322 nm (3.85 eV) respectively. The broad band absorption from 220 nm to 450 nm was due to the electron transition from O^{2-} anti-bonding to the lowest empty orbital of Ce^{4+} that is the electron transition from the valence band to the conduction band [11,13,14]. According to Tauc's law [12], the absorption co-efficient is found to follow the relation

$$(\alpha h\nu)^m = (h\nu - E_g)$$

where α is the absorption coefficient, $h\nu$ is the photon energy, E_g is the band gap energy, $m = 1/2$ or $3/2$ for indirect allowed and indirect forbidden transitions, and $m = 2$ or 3 for direct allowed and direct forbidden transitions. The dependence of $(\alpha h\nu)^m$ on the photon energy $h\nu$ is plotted for different m values. The best fit is obtained for $m = 2$. The band gap energy was estimated by plotting $(\alpha h\nu)^2$

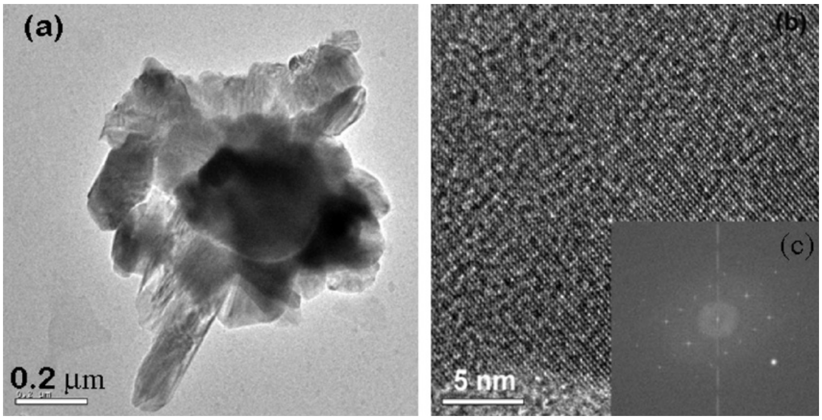

Fig. 2. (a) TEM images of Sr_2CeO_4. (b) The lattice fringe image of Sr_2CeO_4. (c) The inset is the Fast Fourier Transform (FFT) of image (b).

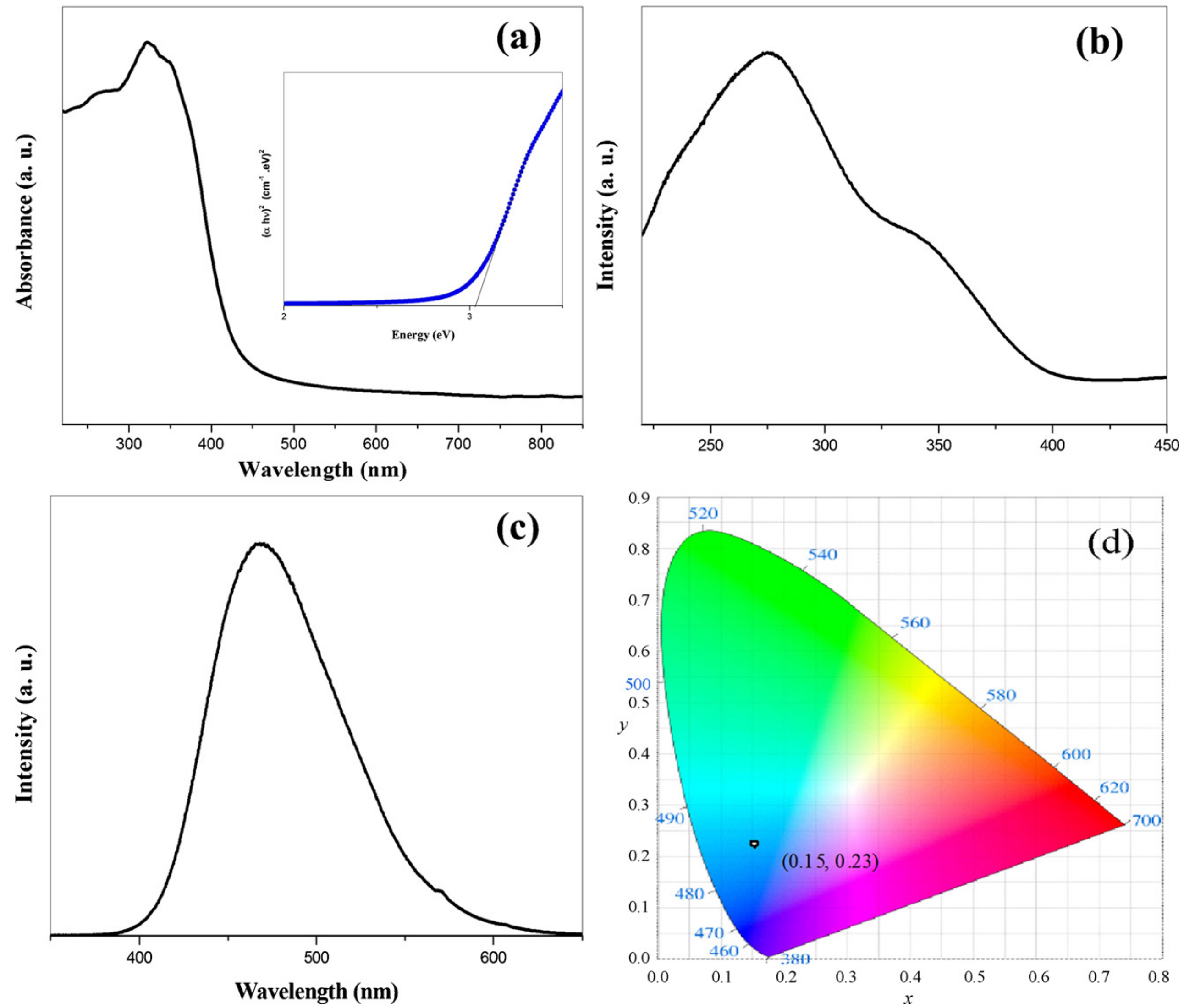

Fig. 3. (a) The absorption, (b) excitation and (c) emission spectra of Sr_2CeO_4. (d) CIE chromaticity diagram of Sr_2CeO_4.

of Sr_2CeO_4 against the photon energy $h\nu$ as shown in the inset of Fig. 3(a). The good relation between $(\alpha h\nu)^2$ and $h\nu$ implies the direct transition of Sr_2CeO_4. The optical band gap energy was determined by extrapolating the linear portion of the plot relating, $(\alpha h\nu)^2$ vs. $h\nu$ to $(\alpha h\nu)^2 = 0$. The band gap energy of Sr_2CeO_4 was determined to be 3.03 eV (410 nm) which is almost in agreement with the reported values, 2.74 eV by Li et al. [13] and 3.2 eV by Goubin et al. [14] using the UV–Vis diffusive reflection spectra.

Fig. 3(b) shows the excitation spectrum of Sr_2CeO_4 with emission fixed at 467 nm. The spectrum displays a broad band which peaks at ~275 nm and has a shoulder at 340 nm. These bands are assigned to the two different Ce^{4+}–O^{2-} distances in the lattice [9]. The excitation band of the sample is attributed to the $t_{1g} \rightarrow f$ transition, where f is the lowest excited CT state of the Ce^{4+} ion and t_{1g} is the molecular orbital of the surrounding ligand in the sixfold oxygen co-ordination [7].

Fig. 3(c) shows the emission spectrum of Sr_2CeO_4 excited at 275 nm. The emission spectrum displays a broad band which peaks at 467 nm [7]. This is assigned to the $f \rightarrow t_{1g}$ transitions of Ce^{4+}. Based on the difference between the first excitation maximum (340 nm) and the emission maximum (467 nm), the Stokes shift is 7998 cm^{-1}, which is within the range of CT transitions on Ce^{4+} ions [11,15,16]. Fig. 3(d) depicts the CIE Diagram 1931, the CIE co-ordinates were calculated by the spectrophotometric method using the spectral energy distribution of Sr_2CeO_4. The color co-ordinates for Sr_2CeO_4 are $x = 0.15$ and $y = 0.23$.

3.3. z-Scan study

Fig. 4 shows the z-scan traces of Sr_2CeO_4. In the z-scan experiment, nanosecond pulses of approximately100 μJ energy were focused using a lens and the sample was translated along the beam axis through the focal region [1]. It is seen that a two-photon absorption (TPA) type process gives the best fit to the obtained experimental data. The z-scan curves obtained are therefore numerically fitted to the nonlinear transmission equation for a two-photon absorption process [17] given by

$$T = \frac{(1-R)^2 \exp(-\alpha L)}{\sqrt{\pi} q_0} \int_{-\infty}^{\infty} \ln[1 + q_0 \exp(-x^2)]\, dx \qquad (1)$$

where T is the transmission of the sample which is defined as the ratio of transmitted and incident energies. R is the Fresnel reflection coefficient at the sample–air interface, and α is the linear absorption coefficient. q_0 is given by $\beta(1-R)I_0L_{\mathrm{eff}}$ where β is the two-photon absorption coefficient, and I_0 is the incident intensity.

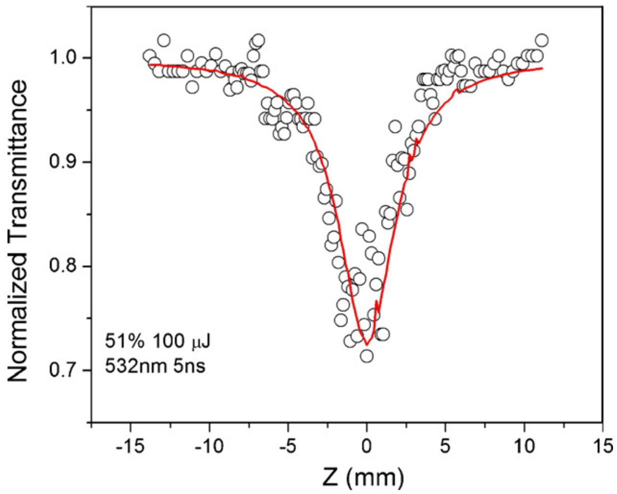

Fig. 4. Open aperture z-scan of Sr_2CeO_4. Circles are data points while the solid curve is a numerical fit using Eq. (1).

L_{eff} is given by $[1-\exp(-\alpha L)]/\alpha$ where L is the sample length. The calculated value for the effective two-photon absorption coefficient is 3.9×10^{-11} m/W. For comparison, under similar excitation conditions, nonlinear optical materials like Cu nanocomposite glasses had given effective TPA coefficient values of 10^{-10}–10^{-12} m/W [18], bismuth nanorods gave 5.3×10^{-11} m/W [19], and CdS quantum dots gave 1.9×10^{-9} m/W [20] respectively. This shows that Sr_2CeO_4 has a comparable optical nonlinearity, so that it can be a potential candidate for optical limiting applications.

4. Conclusions

We have prepared the Sr_2CeO_4 blue phosphor by a solid state reaction method. The XRD study confirms that the structure of the system is orthorhombic. The TEM reveals that Sr_2CeO_4 is composed of elongated spherical structures of length ~0.2–0.6 μm. The FFT of TEM, XRD peaks and the JCPDS values are compared, from which the Sr_2CeO_4 phase is reconfirmed. The excitation spectrum peaks at 275 nm. The emission spectrum displays a peak at 467 nm, which is assigned to the energy transfer between the molecular orbital of the ligand and charge transfer state of the Ce^{4+} ion. The CIE co-ordinates calculated are $x = 0.15$ and $y = 0.23$ respectively, which are in the blue-white region. The measured effective two-photon absorption coefficient is 3.9×10^{-11} m/W, which is comparable to some of the previously measured nonlinear optical materials. This suggests that Sr_2CeO_4 is a suitable material for optical limiting applications.

References

[1] M. Sheik-Bahae, et al., IEEE J. Quantum Electron. 26 (1990) 760–769.
[2] J.G. Tian, et al., Chin. Phys. Lett. 17 (2000) 510.
[3] S.L. Qu, et al., Chin. Phys. Lett. 18 (2001) 1476.
[4] K.P. Unnikrishnan, et al., J. Nonlinear Opt. Phys. Mater. 10 (2001) 113.
[5] O.V. Przhonska, et al., J. Opt. Soc. Am. B 15 (1998) 802.
[6] J. Zhou et al, J. Opt. Soc. Am. B 18 (2001) 1456.
[7] E. Danielson, M. Devenney, D.M. Giaquinta, Science 279 (1998) 837–839.
[8] E. Danielson, et al., J. Mol. Struct. 470 (1998) 229.
[9] R. Sankar, V. Subbha Rao, J. Electrochem. Soc. 147 (7) (2000) 2773–2779.
[10] A. Nag, T.R.N. Kutty, J. Mater. Chem. 13 (2003) 370–376.
[11] L. Van Pieterson, A. Meijerink, J. Alloys Compd. 300 (2000) 426–429.
[12] D.L. Wood, J. Tauc, Phys. Rev. B 5 (8) (1972) 3144–3151.
[13] J. Li, L. Wang, H. Zhou, X. Liu, B. Xu, J. Alloys Compd. 506 (2) (2010) 950–955.
[14] F. Goubin, X. Rocquefelte, M.H. Whangbo, Y. Montardi, R. Brec, S. Jobic, Chem. Mater. 16 (2004) 662–669.
[15] P. Dorenbos, J. Lumin. 111 (2005) 89–104.
[16] P. Dorenbos, J. Phys.: Condens. Matter 15 (2003) 8417–8434.
[17] R.L. Sutherland, Handbook of Nonlinear optics, 2nd edition, Marcel Dekker, New York, 2003 [1996].
[18] B. Karthikeyan, M. Anija, C.S. Suchand Sandeep, T.M. Muhammad Nadeer, R. Philip, Opt. Commun. 281 (2008) 2933.
[19] S. Sivaramakrishnan, V.S. Muthukumar, S. Sivasankara Sai, K. Venkataramanaiah, J. Reppert, A.M. Rao, M. Anija, R. Philip, N. Kuthirummal, Appl. Phys. Lett. 91 (2007) 093104.
[20] P.A. Kurian, C. Vijayan, K. Sathiyamoorthy, C.S. Suchand Sandeep, R. Philip, Nano Res. Lett. 2 (2007) 561.